Lightning climatology of Luxembourg:

A 12-year analysis using Belgium's ground-based lightning location system (BELLS)

Luca MATHIAS

Civil servant's end of internship report

Table of Contents

1. Introduction

Lightning is one of the most striking features of deep moist convection and represents a significant weather hazard across Europe. It is frequently associated with severe phenomena such as heavy rainfall, hail, damaging wind gusts, and tornadoes. Consequently, the study of lightning climatology has become essential not only for advancing meteorological understanding but also for supporting risk management and societal preparedness. The establishment of dense ground-based lightning location systems (LLS) around the globe over the past two decades has enabled the development of detailed climatologies that capture both the spatial distribution and temporal variability of lightning activity with high accuracy.

Several national and pan-European studies have contributed to building a comprehensive picture of lightning occurrence across the continent. In Belgium, Poelman et al. (2014) produced a 10-year climatology using data from the European Cooperation for Lightning Detection (EUCLID). Their analysis revealed mean annual cloud-to-ground (CG) flash densities ranging from 0.3 to 2.4 flashes km^{-2} yr^{-1}, with a strong seasonal concentration between May and August (around 90 % of all flashes) and a pronounced afternoon maximum in the diurnal cycle. This work underscored the importance of long, homogeneous datasets from high-efficiency networks for national-scale assessments. In Germany, Wapler (2013) examined six years of data comprising approximately 36 million strokes at 1 km resolution. The study identified pronounced maxima in southern Germany, particularly in the pre-Alpine region, while minima were observed near the North and Baltic Seas. In Austria, Schulz et al. (2005) analyzed a decade of ALDIS (Austrian Lightning Detection and Information System) data, reporting flash densities between 0.5 and 4 flashes km^{-2} yr^{-1} depending on terrain. Their study also provided detailed statistics on polarity, multiplicity, and peak currents, and demonstrated how improvements in network performance influence climatological results.

Further national-scale climatologies have been established for the Czech Republic (Novák and Kyznarová, 2011), Romania (Antonescu and Burcea, 2010), and Italy (Nicora et al., 2021). On a regional scale, Mäkelä et al. (2014) presented a 10-year statistical analysis of lightning data covering Norway, Sweden, Finland, and Estonia. At the continental level, long-range networks have been used to provide broader context. Anderson and Klugmann (2014), using five years of ATDnet data, produced a European lightning density map that highlighted maxima over the Alps, northern Italy, and the Balkans. Poelman et al. (2016) reported similar results when analyzing data from EUCLID for the period 2006–2014.

Despite this substantial progress, Luxembourg has not yet been the subject of a dedicated lightning climatology. The country's varied topography relative to its small size makes it a particularly interesting case study. Although Luxembourg is occasionally included in broader regional analyses, its lightning characteristics have never been systematically examined at the national scale. This gap is notable given the importance of lightning data for hazard assessment, infrastructure resilience, and climate monitoring (Kühne et al., 2025). It is also especially relevant for the aviation sector: cloud-to-ground discharges pose a direct risk to ground operations at Luxembourg Airport (Findel), where lightning can disrupt refueling, baggage handling, and aircraft servicing, with implications for both safety and operational efficiency.

The present study addresses this gap by presenting a 12-year lightning climatology of Luxembourg, based on observations from Belgium's ground-based lightning location system (BELLS). The analysis focuses specifically on cloud-to-ground lightning discharges, which are of greatest relevance for hazard assessment and operational impacts. The study examines annual, seasonal, and diurnal cycles, evaluates interannual variability and potential long-term trends, and identifies spatial hotspots of lightning occurrence within Luxembourg. In addition, the results are placed in the context of neighboring regions and European-scale climatologies. By establishing the first dedicated lightning climatology for Luxembourg, this work contributes to the broader European literature and provides a reference point for future research on convective activity, severe weather risk, and climate change impacts in the region.

The lightning dataset employed in this study is detailed in Section 2, which also outlines the data-processing procedures used to generate the temporal and spatial analyses. Section 3 presents and interprets the results, and Section 4 concludes the report with a synthesis and discussion of the principal findings.

2. Data and methodology

The data used in this study originates from BELLS established by the Royal Meteorological Institute of Belgium (RMIB) from 2010 onwards with the introduction of Vaisala's Total Lightning Processor (TLP). Beginning in 2011, the network transitioned to low-frequency (LF) LS7001/LS7002 sensors, starting with Ernage (Belgium) and later integrating sensors from France, Germany (DE), the United Kingdom (UK), and the Netherlands (NL) through international cooperation. By 2017, Belgium operated five LF sensors, all upgraded to LS7002 models, with an additional unit installed in northern Luxembourg by MeteoLux and integrated operationally into the network in 2018. Due to the installation of these more performant sensors, the method of lightning detection changed to a time-of-arrival (TOA) and direction-finding (DF) approach, and a significant improvement of intracloud (IC) lightning detection was observed with the sensor upgrade to the LS7002 model (Poelman, 2024).

As of 2024, BELLS consists of 15 LS7002 sensors (Figure 1):

- **5 in Belgium** (Dourbes, Ernage, Koksijde, Oelegem, Riemst, operated by RMIB)
- **5 in different countries via OVE-ALDIS** (DE: Koblenz, Rheine; NL: Ameland, Zandvoort; UK: Norwich) (OVE: Österreichischer Verbund für Elektrotechnik)
- **4 in France** (Deauville, Marcoussis, Mirecourt, Saint-Quentin, operated by Météorage)
- **1 in Luxembourg** (Reuler, operated by MeteoLux; see Figure 2)

With baselines as short as 60–70 km in Belgium and up to 150–200 km at the network edges, BELLS is considered the world's densest LF lightning detection network (Poelman, 2024).

The BELLS dataset used in this study covers the period 2013–2024 and includes, for each detected flash event, the date and time (UTC: Universal Time Coordinated), geographic location (latitude and longitude), peak current (kA), and type (CG or IC). A flash is defined as a group of strokes that are close together in terms of time and space. BELLS uses the following criteria: $\Delta t \leq 1.5$ s and $\Delta r \leq 10$ km. To ensure data quality and minimize the influence of misclassified events, only CG flashes with peak amplitudes ≥ 10 kA or < 0 kA were retained, as positive CG flashes with peak currents below 10 kA are more likely to represent IC flashes (e.g., Biagi et al., 2007; Grant et al., 2012). This filtering step removed a total of 1,080 CG flashes, corresponding to a loss of 6 % of the original CG dataset.

The domain of the data is restricted to the geographical region of the Grand-Duchy of Luxembourg. The spatial analyses were conducted using QGIS (Quantum Geographic Information System), an open-source geographic information system widely applied in

environmental and meteorological studies. Flash density maps were then produced by aggregating the number of retained flashes within each grid cell and normalizing them by the cell's surface area. This approach yields a measure of flash density expressed in flashes per square kilometer, allowing for direct spatial comparison across the study domain.

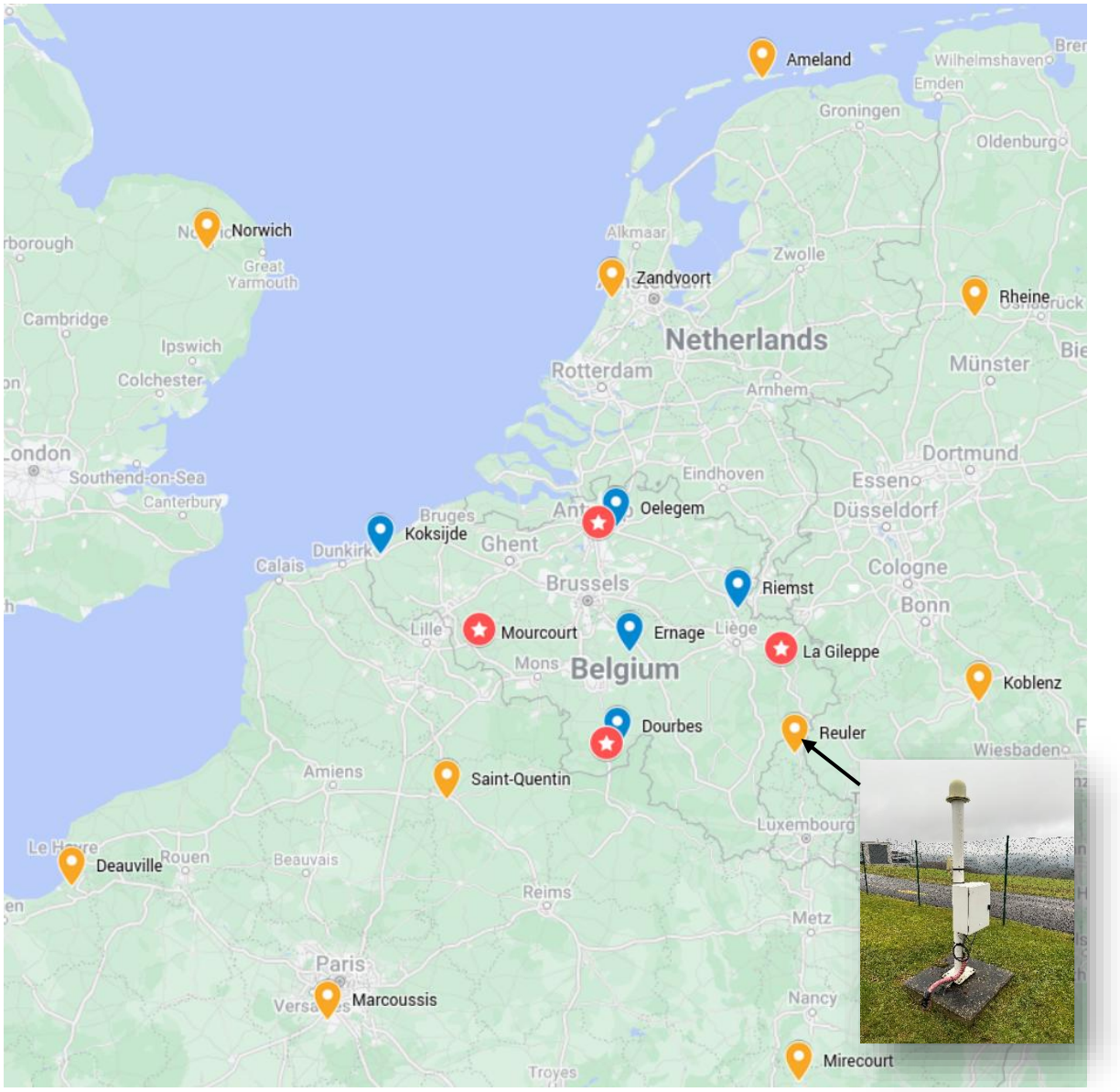

Figure 1. Locations of BELLS sensors. The red markers indicate the decommissioned SAFIR (Surveillance et Alerte Foudre par Interférométrie Radioélectrique) sensors, the blue ones the LS7002 sensors operated by RMIB, and the yellow ones the LS7002 sensors operated by Météorage, OVE-ALDIS, or MeteoLux. Source: Poelman (2024).

3. Results and analysis

3.1 Temporal statistics

Figures 2, 3, and 4 illustrate the temporal distribution of CG flash counts across different time scales for the period 2013–2024 within Luxembourg's borders. In the annual distribution shown in Figure 2, the number of CG flashes exhibits pronounced interannual variability, ranging from a minimum of 678 flashes in 2023 to a peak of nearly 3,700 flashes in 2018. This variability is consistent with previous findings for Belgium (Poelman, 2014; Poelman, 2024) and can be attributed to fluctuations in mesoscale and synoptic-scale conditions that modulate thunderstorm occurrence. The 12-year mean amounts to 1,126 flashes, underscoring 2018 as a distinct outlier (see Table A3) and identifying it as an exceptionally active thunderstorm season across both Luxembourg and Belgium (Poelman, 2024).

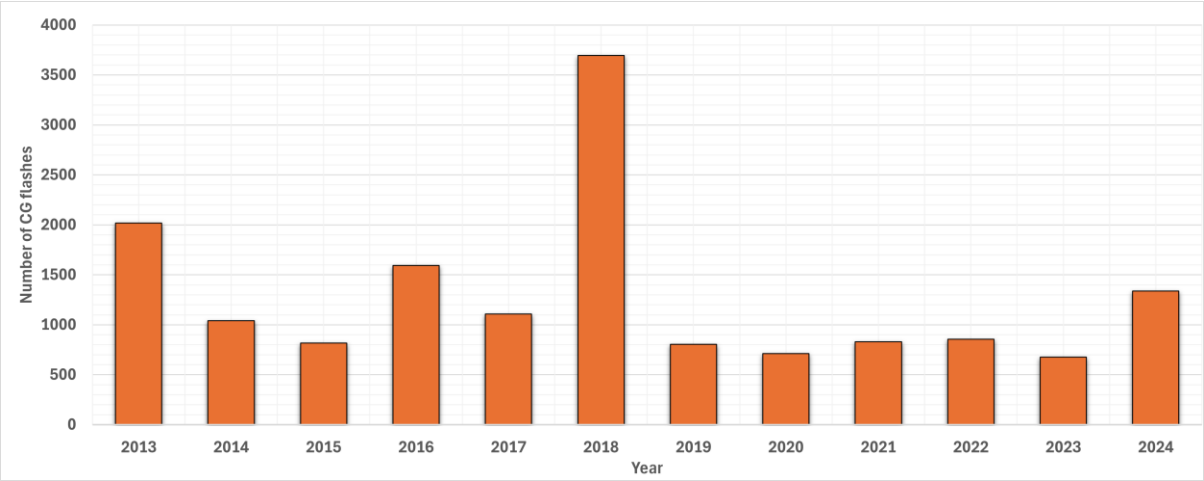

Figure 2. Annual counts of cloud-to-ground flashes based on BELLS data.

The monthly distribution of CG flashes is presented in Figure 3. Nearly 85 % of the electrical activity occurs between May and August, with a pronounced peak in June. This concentration can be attributed to strong solar radiation and the near-surface advection of moist air, which together yield elevated values of convective available potential energy (CAPE) (Taszarek et al., 2020a). Previous studies (Taszarek et al., 2020a, 2020b; Poelman, 2014, 2016) indicate that lightning activity across Central Europe typically peaks in July. However, the BELLS dataset reveals a different pattern for Luxembourg. One possible explanation is that, over a small domain such as Luxembourg (2,586 km²), a single day or multiple days of intense convective activity can disproportionately influence the monthly or even annual totals.

By contrast, the period from October to March contributes only about 2 % of the observed flashes. Thunderstorms during late autumn and winter are generally associated with the passage of cold fronts or post-frontal conditions, and they tend to be short-lived.

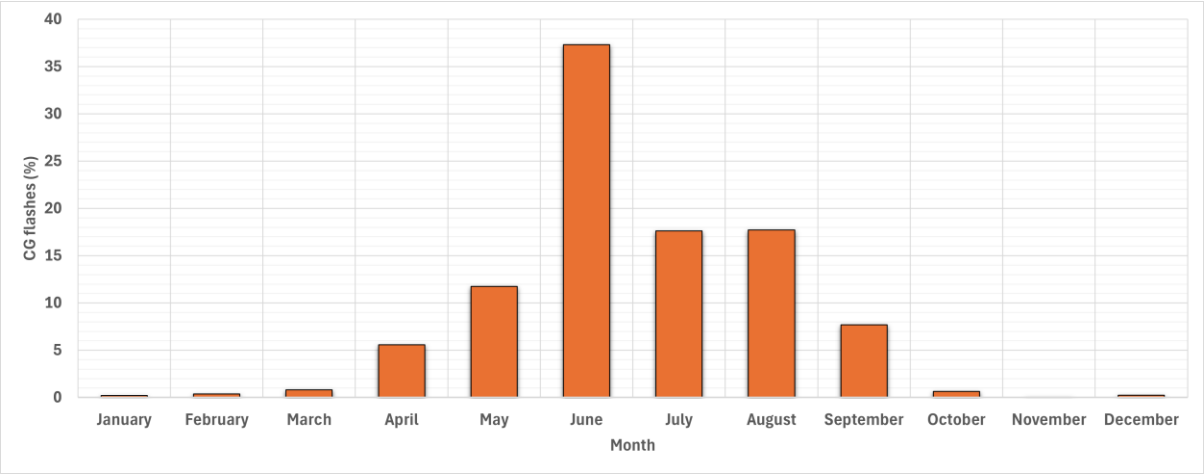

Figure 3. Mean monthly counts of cloud-to-ground flashes based on BELLS data for the period 2013-2024.

Figure 4 shows the diurnal distribution of CG flash counts, resolved at a 1-hour interval (HH:00–HH:59) and expressed as a percentage of the total activity. A minimum occurs during the morning hours, followed by a steady increase from 11:00 UTC onward, reaching a pronounced maximum between 16:00 and 19:00 UTC. A secondary, shorter-lived peak is evident between 20:00 and 21:00 UTC. Overall, about 67 % of the flashes are concentrated between 14:00 and 21:00 UTC. This diurnal cycle is primarily driven by solar heating of the surface, which favors the initiation of deep moist convection. A marked decline in activity is only observed after 22:00 UTC. This delayed decrease is likely associated with long-lived convective systems originating in France that become elevated as they propagate into Luxembourg from southwesterly directions. The overall diurnal pattern aligns closely with observations from other European regions (e.g., Antonescu and Burcea, 2010; Wapler, 2013; Poelman, 2014).

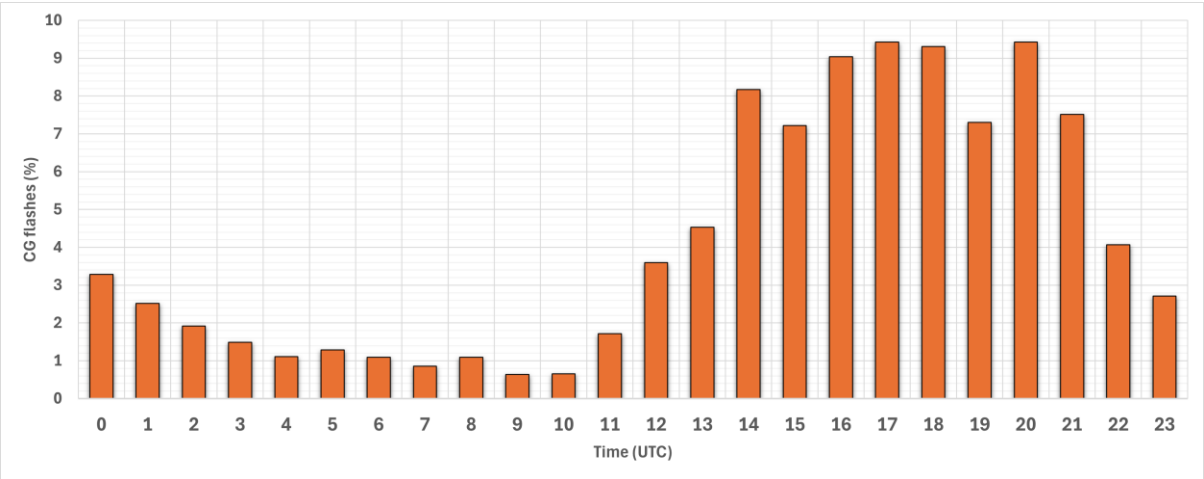

Figure 4. Mean diurnal counts of cloud-to-ground flashes based on BELLS data for the period 2013–2024. Note that local time is UTC + 1 h and + 2 h in winter and summer, respectively.

3.2 Flash characteristics

In this section, the polarity and peak currents of CG flashes are examined. Figure 5 presents the monthly mean polarity distribution for Luxembourg. Overall, 10 % of the observed flashes are positive, a proportion comparable to findings from Austria (Schulz et al., 2005) and Belgium (Poelman, 2014), but markedly lower than reported for Germany (Wapler, 2013). The anticipated increase in positive flashes during winter, typically attributed to the reduced vertical extent of thunderstorm clouds (Takagi et al., 1986; Pinto et al., 1999a), was not observed in Luxembourg. This contrasts with the aforementioned studies, which captured such a seasonal pattern. The low fraction of positive flashes during the cold season is likely an artifact of the limited sample size of CG flashes.

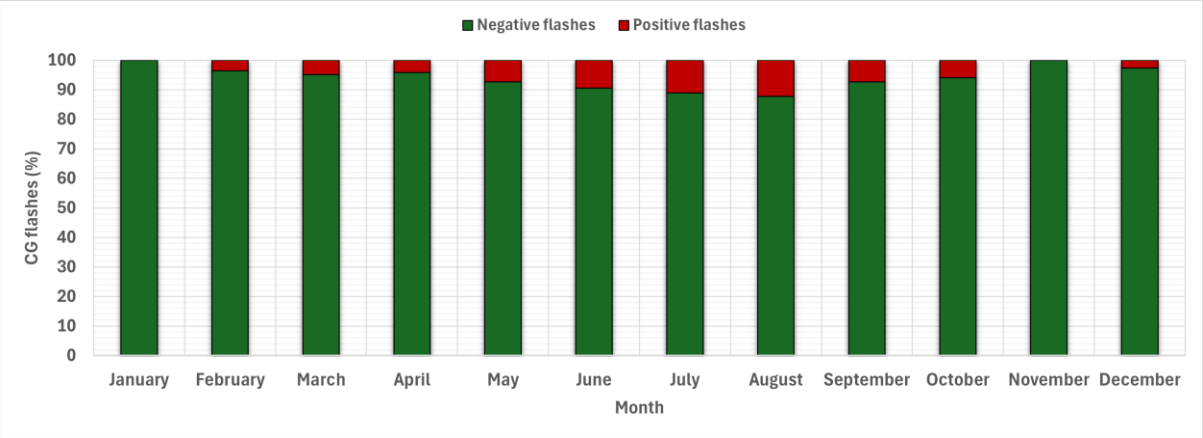

Figure 5. Mean monthly polarity distribution of CG flashes based on BELLS data for the period 2013–2024.

Regarding the amplitude of CG flashes, the mean estimated peak currents in Luxembourg are -12.9 kA for negative flashes and +42.7 kA for positive ones. This polarity-dependent signature is clearly reflected in the cumulative statistical distribution shown in Figure 6, which displays the percentage of absolute peak currents exceeding a given value along a logarithmic horizontal axis. The vertical axis is scaled such that the distribution approximates a slanted straight line, facilitating interpretation. From this representation, one can infer that approximately 50% of negative flashes exceed 8 kA, while for positive flashes, this threshold rises to 29 kA. Moreover, negative flashes with amplitudes above 100 kA are considerably rarer than their positive counterparts. The highest estimated peak current recorded in Luxembourg during the period 2013–2024 was +342 kA. These findings are consistent with earlier studies by Poelman (2014) and Poelman et al. (2016).

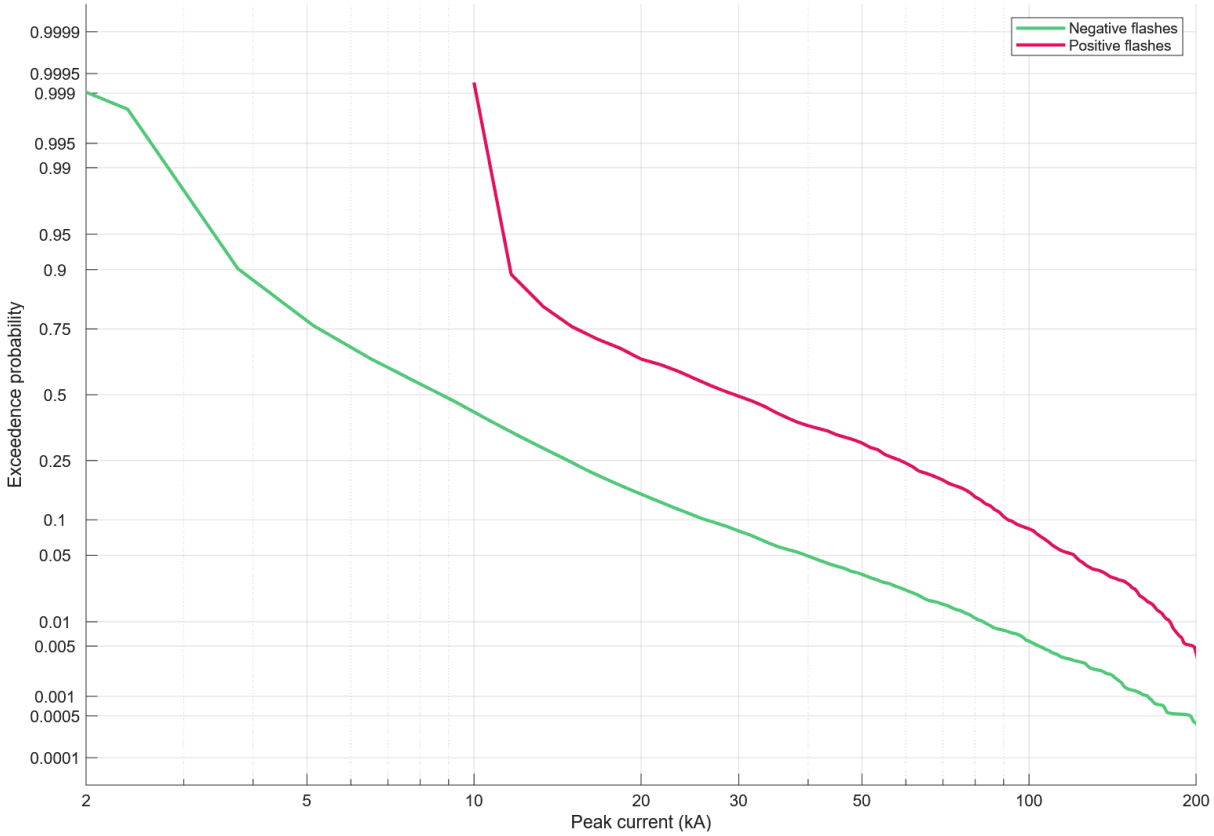

Figure 6. Cumulative statistical distribution of peak currents (in kA) for negative CG flashes (green) and positive CG flashes (red) based on BELLS data for the period 2013–2024.

3.3 Flash density

Figure 7a illustrates the spatial distribution of the mean annual CG flash density, N_g (in km^{-2} yr^{-1}), derived from a dataset of 15,494 CG flashes. The analysis was conducted at a spatial resolution of 1 km × 1 km, which is appropriate given the location accuracy of the BELLS detection system (approximately 100 to 200 m). The resulting map reveals a heterogeneous and somewhat noisy distribution, with values spanning a broad range across Luxembourg. The countrywide mean CG flash density is approximately 0.5 km^{-2} yr^{-1}, slightly below the value found for Belgium by Poelman (2014). When placed in a global context, the flash density observed in Luxembourg can be considered moderate. Densities in certain regions of the United States, South America, Central Africa, and other lightning-prone areas frequently exceed the maximum values observed in Luxembourg by at least one order of magnitude.

Interestingly, three localized hotspots of elevated CG flash density emerge, each associated with tall man-made structures (Figure 8). These include the radio antennas in Dudelange (285 m AGL) and Hosingen (300 m AGL), as well as a wind turbine northwest of Ettelbruck (142.5 m AGL). The influence of these structures is evident in the markedly higher flash densities recorded in their vicinity. The Dudelange tower exhibits the highest value, with N_g = 3.3 km^{-2} yr^{-1}, followed by Hosingen with N_g = 2.4 km^{-2} yr^{-1}. Such localized enhancements underscore the role of tall conductive objects in modulating lightning density and highlight the importance of considering both natural and anthropogenic factors in lightning climatology.

One effective way to reduce the noisiness of the CG flash density field is through spatial smoothing. In practice, this involves calculating, for each location within the 1 km × 1 km grid, the number of CG flashes recorded within a specified radius and assigning the mean value within that circle as the representative flash density at that position. Figure 7b illustrates this approach using a radius of 5 km. The method substantially reduces the highly variable nature of N_g while preserving the broader spatial trends. The smoothed distribution reveals subtle but distinct regional contrasts across Luxembourg. Elevated flash densities are evident in the vicinity of Dudelange, Esch-sur-Alzette, Hosingen, Luxembourg City, and within the forested area known as Biischtert, west of Colmar-Berg. In contrast, the lowest densities are concentrated along the Moselle valley in the southeast. It should be noted, however, that localized anomalies may arise from the occurrence of individual intense storms and the inherent variability of thunderstorm activity. These factors can imprint short-term fluctuations on the spatial pattern, even when long-term averages are considered.

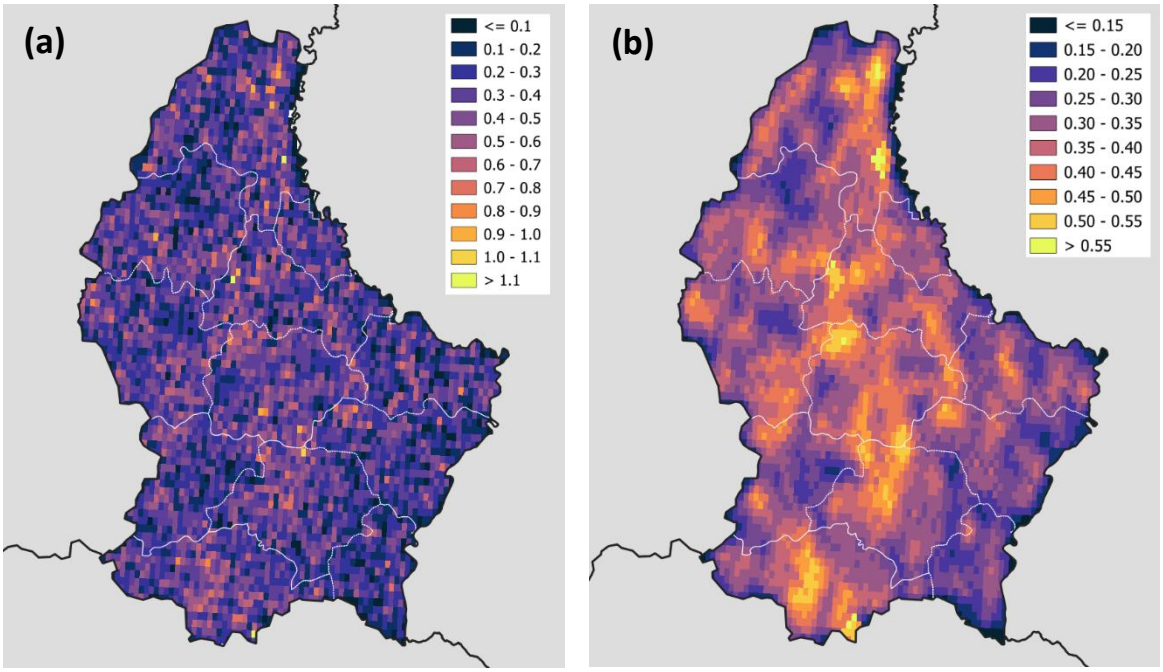

Figure 7. (a) Spatial distribution of the mean annual CG flash density (in km^{-2} yr^{-1}) adopting a spatial resolution of 1 km x 1 km. (b) Same as in (a) but taking the mean value in a 5 km radius. The dotted white lines denote the borders of the cantons.

Figure 8. Radio antennas in Dudelange and Hosingen, respectively, and the wind turbine to the northwest of Ettelbruck (from left to right). The source of the background is the most recent orthophotography taken from geoportail.lu and the orange dots indicate the location of the CG flashes based on BELLS data for the period 2013–2024. The detected flash location is slightly offset from the actual point of impact (on average 75 to 150 m), which is an indication of the location accuracy of BELLS.

Despite this variability, practical use cases often require a simplified representation of lightning activity. In many cases, the public or enquirer is primarily interested in lightning activity within a specific commune or canton. For such applications, it is preferable to assign a single representative value to each administrative unit. This approach is illustrated in Figure 9, where the flash density for each canton and commune is calculated by summing all recorded flashes within its boundaries and dividing by the respective area.

At the canton level (Figure 9a), the resulting distribution closely resembles the smoothed flash densities presented in Figure 7b. The lowest mean annual CG flash density is found in Remich, located in southeastern Luxembourg, with $N_g = 0.38$ km^{-2} yr^{-1}. The highest values occur in Esch-sur-Alzette and Mersch, both with $N_g = 0.56$ km^{-2} yr^{-1}.

On the communal scale (Figure 9b), the lowest density is observed in Wormeldange along the Moselle valley ($N_g = 0.29$ km^{-2} yr^{-1}). In contrast, the communes of Schifflange ($N_g = 0.76$ km^{-2} yr^{-1}), Dudelange ($N_g = 0.74$ km^{-2} yr^{-1}), Lorentzweiler ($N_g = 0.72$ km^{-2} yr^{-1}), and Heffingen ($N_g = 0.71$ km^{-2} yr^{-1}) exhibit the highest densities. It should be noted, however, that the value for Dudelange is strongly influenced by the presence of a radio antenna within the commune, which enhances local CG lightning probability.

The complete ranking of the cantons and communes can be found in the annex (Tables A1 and A2).

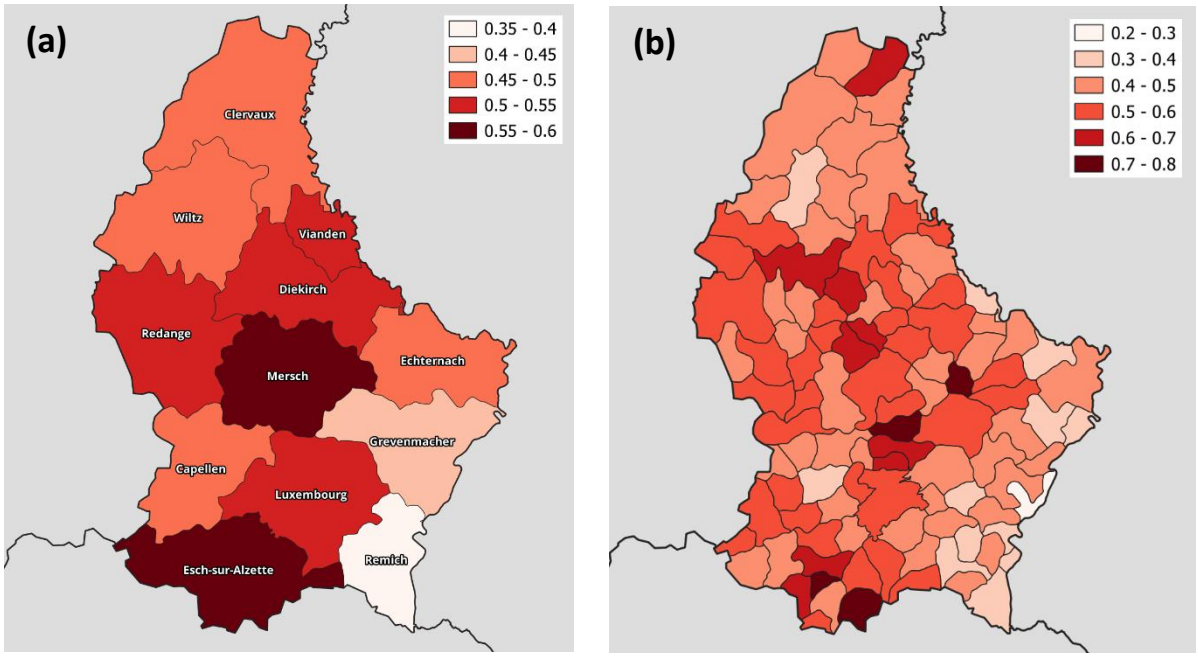

Figure 9. CG flash densities (in km^{-2} yr^{-1}) for each (a) canton and each (b) commune based on BELLS data for the period 2013–2024.

Assessing lightning strike density in the vicinity of airports is of particular importance, given the potential implications for ground operations, infrastructure safety, and operational continuity. For example, during a thunderstorm on the evening of 22 July 2013, a CG lightning flash (-16 kA) was registered near the wind measurement system located at the middle along the runway, leading to a data outage and no wind information in the METAR (Meteorological Aerodrome Report) message for approximately eight hours (see annex, Figure A1), posing a safety risk to aircraft operations. For Airport Luxembourg-Findel, the analysis was conducted by calculating the mean annual CG flash density within the airport perimeter, extended by a 500 m buffer zone to account for nearby strikes that may still pose operational risks (Figure 10).

Over the 12-year observation period, BELLS recorded a total of 62 CG flashes (5.17 CG flashes per year) within this buffered area. This corresponds to an average flash density of $N_g = 0.51$ km^{-2} yr^{-1}, which is consistent with the national mean. Because the dataset spans only 12 years and shows strong overdispersion (variance/mean ≈ 9.35), parametric models such as the Poisson distribution are not appropriate for estimating the probability of occurrence and return periods for ≥ k CG flashes. A purely empirical approach therefore provides the most reliable basis for operational decision-making in the airport environment. The empirical distribution shows that lightning occurs in 83% of years, meaning that at least one CG flash within the airport area is a near-annual event with potential implications for ground operations. Overall, low-to-moderate lightning activity is the most common operational scenario according to this dataset. There are no years with a CG flash amount between 6 and 16, while a few isolated high-activity years (17 and 22 flashes) are evident (see Figure 11). These rare but intense years are the ones most likely to trigger extended ground stops, and repeated lightning-alert activations. Because return periods are computed as $T(k) = 1/P(X \geq k)$, thresholds exceeded in the same number of years share identical return periods. This produces the observed step-like structure: any threshold between 6 and 16 flashes corresponds to a 6-year return period because only two years exceeded all these values. Operationally, this means that while most years show only a handful of CG flashes, the airport must remain prepared for occasional seasons with substantially elevated lightning activity, even if such years are infrequent.

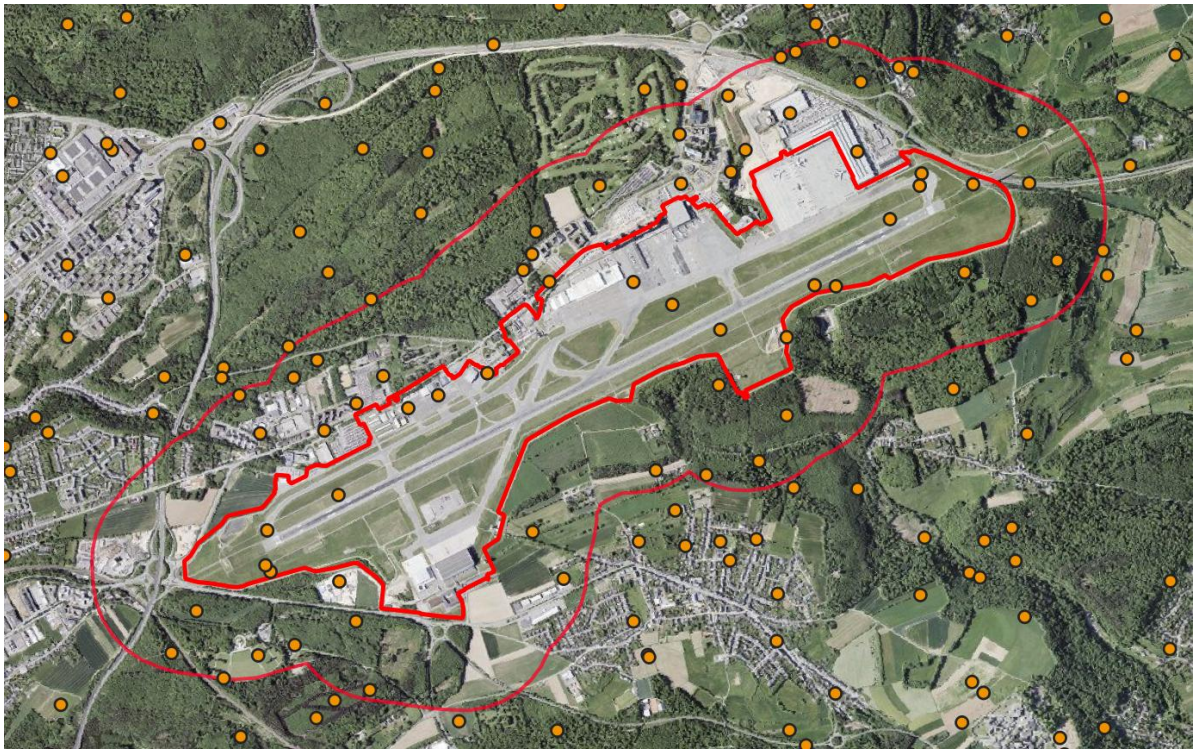

Figure 10. The thick red line denotes the perimeter of the Airport Luxembourg-Findel, whereas the thin red line marks the 500 m buffer zone. The source of the background is the most recent orthophotography taken from geoportail.lu and the orange dots indicate the location of the CG flashes based on BELLS data for the period 2013–2024.

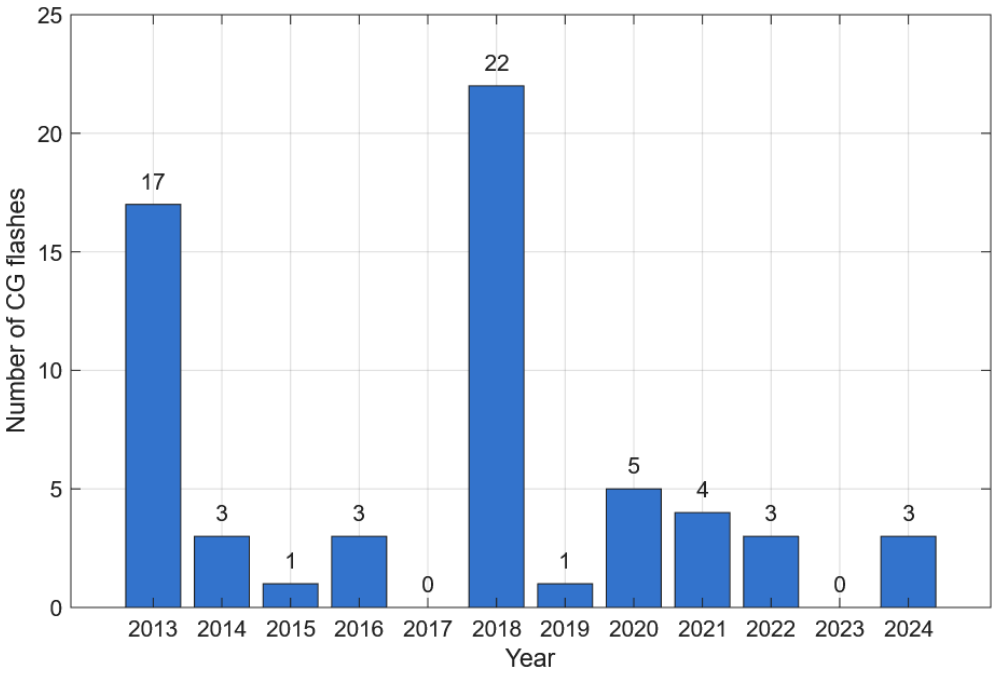

Figure 11. Annual counts of CG flashes for the perimeter of the Airport Luxembourg-Findel, as described in Figure 10.

3.4 Thunderstorm days

To evaluate the climatology of thunderstorm days (T_d) in Luxembourg, human observations from Luxembourg-Findel Airport were taken as the reference dataset and systematically compared against the BELLS lightning detection records for the 12-year period 2013–2024. Since audible thunder depends on proximity, BELLS data was analyzed using three spatial thresholds: 8 km, 12 km, and 16 km around Findel. The 8 km and 16 km radii correspond directly to the operational criteria used in METAR reporting, while the intermediate 12 km radius was included to provide an additional sensitivity test. The comparison results are presented in Figure 12. They demonstrate that the 16 km radius reproduces the observed thunderstorm day climatology most closely. Over the 12-year period, the average number of thunderstorm days recorded at Findel was 20.4, while the BELLS dataset within a 16 km radius yielded a nearly identical mean of 20.9. By contrast, the smaller radii systematically underestimate thunderstorm occurrence: the 8 km radius produced an average of 13.2 days, and the 12 km radius yielded 17.6 days (see Figure 12).

This analysis highlights the importance of radius selection when translating lightning detections into thunderstorm day climatologies. While smaller radii capture only the most local events, the 16 km threshold aligns well with the operational definition of audible thunder and provides the most representative match to human observations at Luxembourg-Findel. This outcome contrasts with the findings of Tuomi (2001) and Bourscheidt et al. (2012), who reported the smallest biases relative to human observations at radii considerably below 16 km. A plausible explanation for this discrepancy lies in regional characteristics such as topographic exposure, ambient noise conditions, and altitude, which can influence the effective range of audible thunder and thus the correspondence between lightning detections and observed thunderstorm days.

Using the ratio between thunderstorm days (T_d) and CG flash density (N_g) derived for Luxembourg-Findel Airport ($T_d/N_g = 40$), the yearly average number of T_d was estimated for each of the 12 cantons based on their respective annual CG flash densities. The resulting 12-year climatology indicates a range from approximately 15 to 22 days across Luxembourg. These values are consistent with the thunderstorm day frequencies reported for Belgium by Poelman (2014), supporting the robustness of the scaling approach across the region.

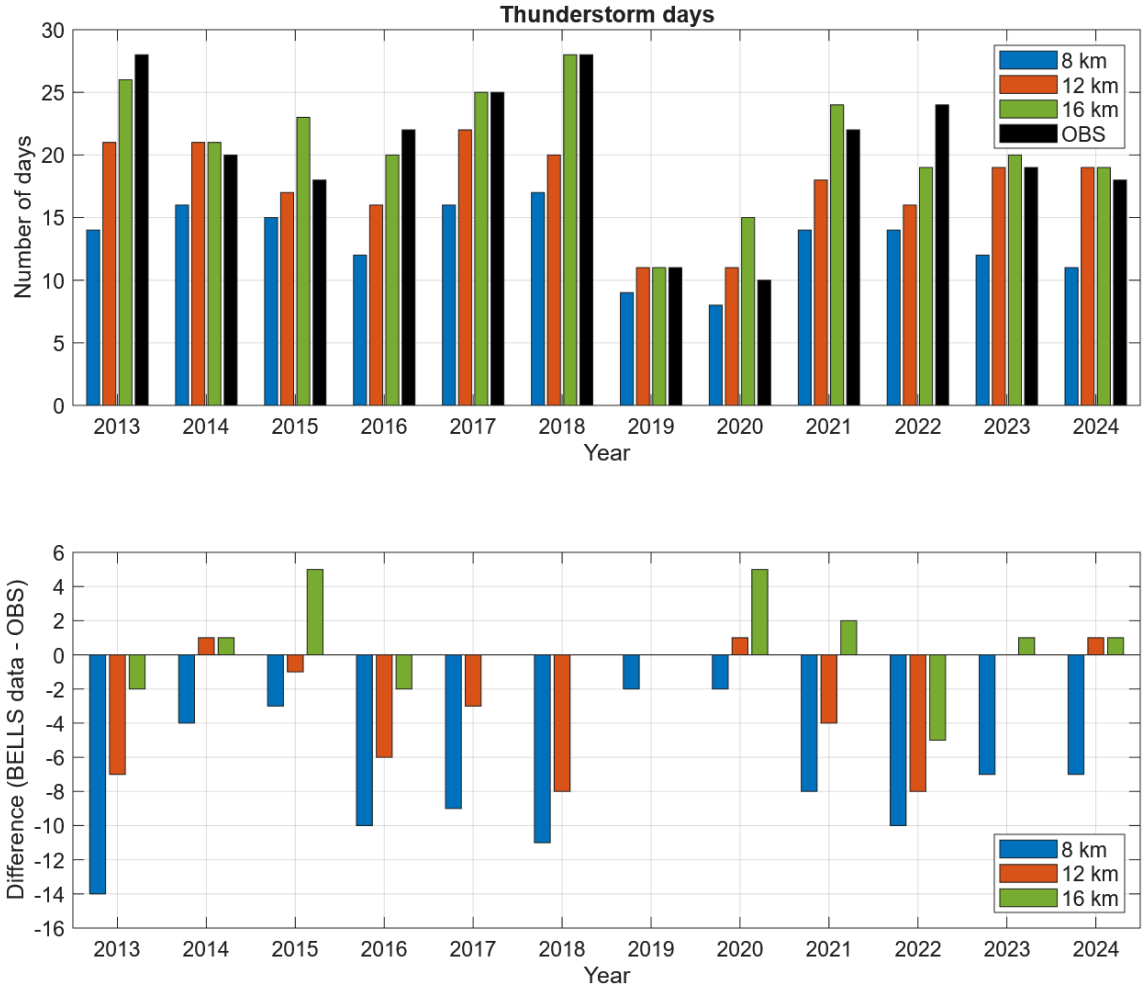

Figure 12. Comparison of thunderstorm day climatologies derived from BELLS lightning detections at varying radii (8 km, 12 km, 16 km) against human observations (OBS) at Airport Luxembourg-Findel (2013–2024).

3.5 Intracloud lightning

Since 2018, the BELLS network has provided robust detection of IC lightning following the full transition to LS7002 sensors. This upgrade markedly enhanced the system's sensitivity to the higher-frequency electromagnetic signatures characteristic of IC discharges, yielding a more complete representation of total lightning activity across the region (Poelman, 2024). Over the period 2018–2024, BELLS detected 44,728 IC flashes within Luxembourg's borders, a total that includes positive CG flashes with peak currents ≤ 10 kA reclassified as IC to account for known misidentification biases (see section 2).

The relative contributions of IC and CG flashes to total lightning are presented in Figure 13. IC flashes consistently dominate the electrical activity, accounting for approximately 70–90 % of all detected flashes. From 2020 onward, IC flashes outnumber CG flashes by an average factor of 7.8, underscoring the dominant role of IC lightning as an indicator of storm electrification and overall thunderstorm activity in Luxembourg. In the preceding two years (2018–2019), the mean IC/CG ratio was considerably lower at 2.5. This marked increase coincides with the discontinuation of the older SAFIR sensors in 2020, which had previously contributed to IC identification within BELLS (Poelman, 2024) and likely reflects the improved consistency and sensitivity of the network's IC detection capability following their removal.

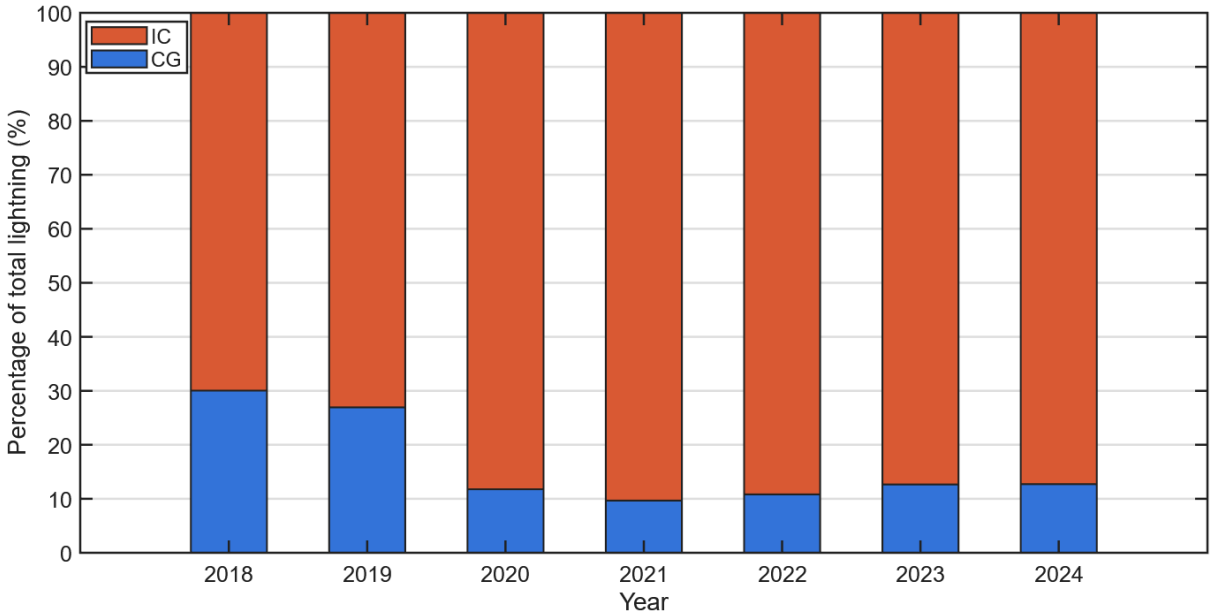

Figure 13. Annual relative contribution of CG and IC flashes to total lightning based on BELLS data for the period 2018–2024.

The monthly distribution of the relative CG/IC contribution shows that IC flashes are less dominant during the cold season (Figure 14). This behavior reflects the strong dependence of IC lightning on the depth of the mixed-phase region of thunderstorm clouds and the intensity of the updraft – both of which are closely tied to atmospheric instability. Since instability is typically greatest during the warm season (April to September), IC flashes become increasingly prevalent during this period, whereas their relative contribution decreases during the cooler months.

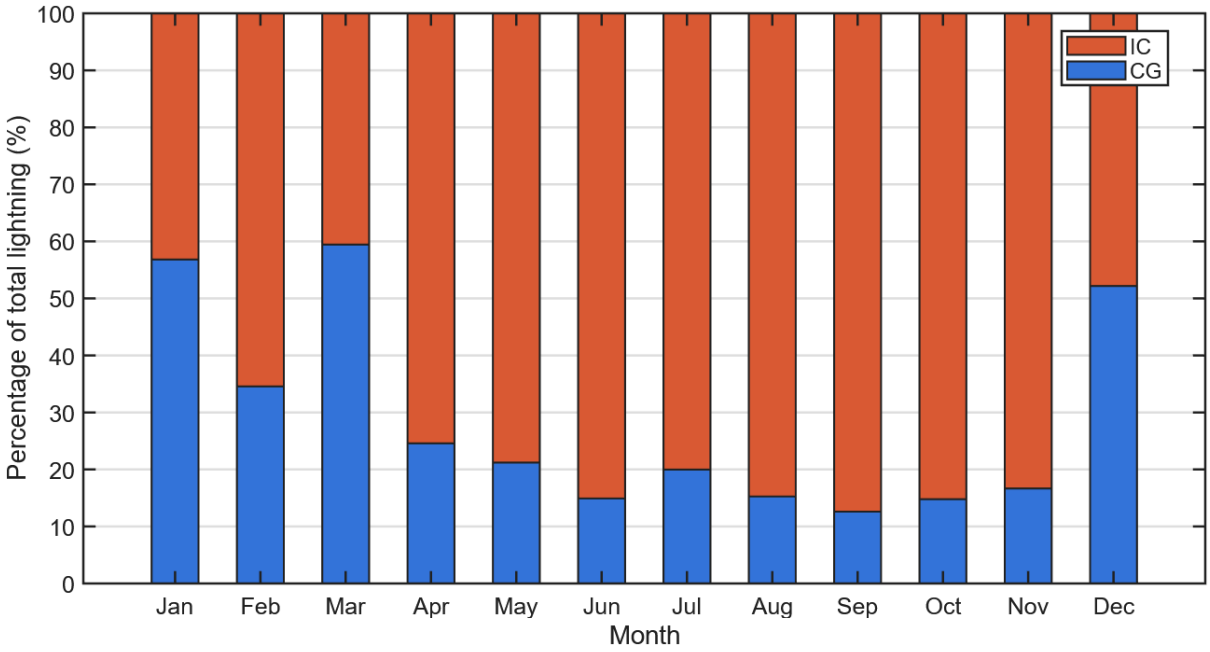

Figure 14. Monthly relative contribution of CG and IC flashes to total lightning based on BELLS data for the period 2018–2024.

Figure 15 presents the mean annual IC flash density for the period 2018–2024. Compared to the CG flash density map (Figures 7 and 9), the IC distribution is noticeably smoother and exhibits fewer localized maxima. The highest IC densities occur broadly across northern Luxembourg, while the only region where IC densities resemble the CG pattern is the Moselle valley, where both datasets show the lowest values. This alignment reflects the limited convective activity typically observed along the Moselle corridor.

Elsewhere, the spatial patterns diverge more clearly. IC densities show a pronounced northwest to southeast gradient, with elevated values across the Oesling and lower values toward the southeast. This contrasts with the CG flash density, which placed greater emphasis on central and southern Luxembourg. The broader and more coherent IC footprint is consistent with the influence of terrain: convective initiation and sustained storm development are often favored in more elevated and heterogeneous landscapes (Kottmeier et al., 2008; Hagen et al., 2011; Cummins, 2014), which in Luxembourg are primarily located in the north and west. Comparable results have been reported for Belgium (Poelman, 2024).

Overall, IC lightning provides a more complete and physically representative picture of thunderstorm activity. IC flashes typically precede CG flashes in the storm life cycle and are less affected by man-made structures or local triggering effects, making them a more reliable indicator of storm electrification and convective intensity. Thus, incorporating IC lightning information may also strengthen operational decision-making in airport environments.

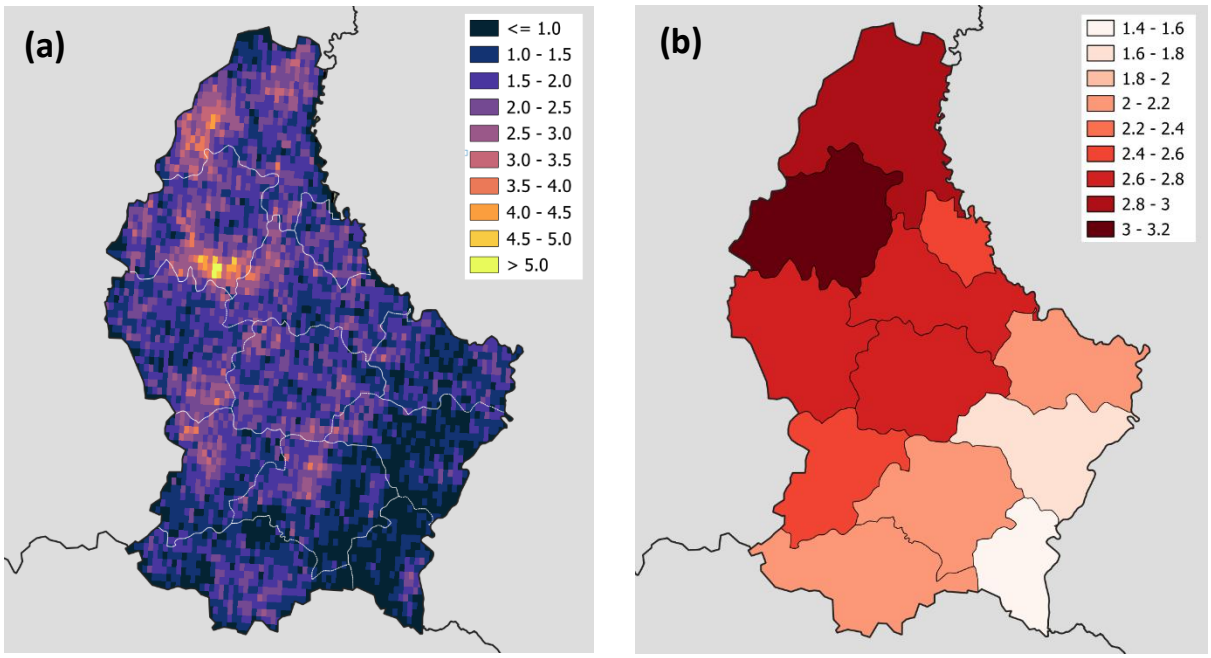

Figure 15. (a) Spatial distribution of the mean annual IC flash density (in km^{-2} yr^{-1}) adopting a spatial resolution of 1 km x 1 km. The dotted white lines denote the borders of the cantons. (b) IC flash densities (in km^{-2} yr^{-1}) for each canton commune based on BELLS data for the period 2018–2024.

4. Discussion and conclusions

This study provides the first comprehensive assessment of lightning activity in Luxembourg and offers new insights into the country's convective climate. The temporal analyses reveal a strong concentration of lightning in the warm season and a pronounced late afternoon maximum, reflecting the dominant role of surface heating and boundary-layer destabilization. Interannual variability is considerable, with individual high-impact convective episodes exerting a strong influence on annual totals due to the small size of the domain.

Spatially, CG flash densities show a heterogeneous pattern shaped by both natural and anthropogenic factors. Localized maxima near tall structures highlight the sensitivity of CG lightning to artificial triggering, while broader terrain-related gradients emerge only after spatial smoothing. These limitations become evident when comparing CG and IC flash densities: IC lightning produces a more coherent and physically meaningful spatial structure, with a clear northwest to southeast gradient and consistently low values along the Moselle valley.

A purely empirical analysis of annual CG flashes within a buffer for the Airport Luxembourg-Findel shows that CG lightning occurs in 83% of years, making at least one event a near-annual operational consideration. Overall, the empirical return-period curve captures the following behavior of lightning within the airport buffer: frequent low-impact years, occasional moderate years, and rare but operationally significant high-activity events. These results highlight the episodic nature of convection specifically at the airport and the need for consistent lightning-alert readiness. 30 years of data would allow an even more robust statistical analysis.

The integration of IC lightning into the climatology represents a major advancement. With the improved IC detection capability of BELLS following the transition to LS7002 sensors, IC flashes now provide a more complete depiction of storm electrification. Their inclusion offers several key benefits for understanding convective behavior in Luxembourg:

- They capture weak or elevated storms that may produce few or no CG flashes.
- Their higher frequency yields more stable temporal statistics and reduces the influence of local triggering by tall structures.
- Their spatial distribution is smoother and less noisy, revealing broader convective patterns.
- They offer better insight into storm life cycles, particularly during initiation and decay phases.
- They provide operational value, as IC activity often increases earlier than CG activity and can serve as an early indicator of storm intensification.

Beyond these advantages, IC lightning is also central to the detection of lightning jumps, which are rapid increases in total lightning activity that signal strengthening updrafts and the potential onset of severe weather. Because lightning jumps are driven by changes in storm electrification aloft, they are far more evident in IC activity than in CG flashes. This makes IC lightning a key diagnostic for identifying intensifying convection, particularly during the early stages of storm development when CG activity may still be limited. The ability to monitor lightning jumps therefore enhances both scientific understanding and operational nowcasting capabilities (Erdmann and Poelman, 2023).

Looking ahead, the advent of the Meteosat Third Generation Lightning Imager (MTG-LI) will further strengthen lightning monitoring over Luxembourg and the broader European region. The MTG-LI provides continuous, full-disk detection of optical lightning emissions from geostationary orbit, capturing both IC and CG activity with high temporal resolution. Its independent, uniform coverage offers a valuable external reference for BELLS and enables cross-validation of detection efficiencies (e.g., Van der Velde et al., 2024). Importantly, the MTG-LI's ability to track rapid fluctuations in total lightning activity, including lightning jumps, will improve early identification of rapidly intensifying convection, supporting aviation, civil protection, and severe weather warnings.

Maintaining and regularly updating this lightning climatology will be essential for monitoring how convective behavior evolves in Luxembourg over the coming decades. As BELLS continues to operate with a stable sensor configuration and as new observational platforms such as the MTG Lightning Imager become fully integrated, future updates will allow for the detection of long-term trends, shifts in storm seasonality, and potential changes in thunderstorm frequency or intensity linked to a warming climate. A sustained climatological record will also support improved risk assessments for infrastructure, aviation, and civil protection. Continued monitoring is therefore not only scientifically relevant but also operationally important for understanding how convective hazards may evolve in Luxembourg's changing climate.

In summary, this climatology establishes a robust baseline for understanding convective behavior in Luxembourg. It demonstrates the value of combining CG and IC lightning data, highlights the influence of terrain and infrastructure on lightning occurrence, and underscores the operational relevance of total lightning monitoring. The findings provide a foundation for future research on severe weather, long-term convective variability, and the evolving convective regime in the region, particularly as new observational capabilities such as the MTG Lightning Imager become fully integrated into operational workflows.

Acknowledgements

I wish to express my gratitude to Dr. Dieter Poelman (RMIB) for providing the lightning data essential to the development of this report and for his feedback.

I also extend my sincere appreciation to my main reviewers, Dr. Joerg Bareiss and Aline Freyermuth (MeteoLux), whose insightful comments and constructive evaluations contributed to the refinement and clarity of this report.

Finally, I would like to convey my deepest thanks to my wife, whose encouragement, and support have been invaluable throughout the process of writing this report.

References

Anderson, G., and D. Klugmann, 2014: A European lightning density analysis using 5 years of ATDnet data. *Nat. Hazards Earth Syst. Sci.*, **14**, 815–829.

Antonescu, B., and S. Burcea, 2010: A cloud-to-ground lightning climatology for Romania. *Mon. Wea. Rev.*, **138**, 579–591.

Biagi, C. J., et al., 2007: National Lightning Detection Network (NLDN) performance in southern Arizona, Texas, and Oklahoma in 2003–2004. *J. Geophys. Res.*, **112**, D05208.

Bourscheidt, V., et al., 2012: Methods to overcome lightning location system performance limitations on spatial and temporal analysis: Brazilian case. *J. Atmos. Oceanic Technol.*, **29**, 1304–1311.

Cummins, K., 2014: Mapping the impact of terrain on lightning incidence and multiple ground contacts in cloud-to-ground flashes. *Proc. 15th Int. Conf. on Atmospheric Electricity*, Norman, OK, ICAE, 16 pp. [Available online at http://www.nssl.noaa.gov/users/mansell/ icae2014/preprints/Cummins_68.pdf]

Erdmann, F., and D. R. Poelman, 2023: Automated Lightning Jump (LJ) detection from geostationary satellite data. *J. Appl. Meteor. Climatol.*, **62**, 1573–1590.

Grant, L. D., et al., 2012: Positive polarity: Misclassification between intracloud and cloud-to-ground discharges in the Southern African Lightning Detection Network. *Proc. 22nd Int. Lightning Detection Conf.*, Broomfield, CO, Vaisala, 5 pp. [Available online at https://www.vaisala.com/sites/default/files/documents/Positive%20Polarity.pdf]

Hagen, M., et al., 2011: Influence of the wind profile on the initiation of convection in mountainous terrain. *Quart. J. Roy. Meteor. Soc.*, **137**, 224–235.

Kottmeier, C., et al., 2008: Mechanisms initiating deep convection over complex terrain during COPS. *Meteor. Z.*, **17**, 931–948.

Kühne, T., et al., 2025: Lightning fatalities in Europe (2001–20). *Wea. Climate Soc.*, **17**, 205–215.

Mäkelä, A., et al., 2014: Nordic lightning information system: Thunderstorm climate of Northern Europe for the period 2002–2011. *Atmos. Res.*, **139**, 46–61.

Nicora, M. G., et al., 2021: A 10-year study on the lightning activity in Italy using data from the SIRF network. *Atmos. Res.*, **256**, 105552.

Novák, P., and H. Kyznarová, 2011: Climatology of lightning in the Czech Republic. *Atmos. Res.*, **100**, 318–333.

Pinto, O., Jr., et al., 1999a: Cloud-to-ground lightning in southeastern Brazil in 1993: 1. Geographical distribution. *J. Geophys. Res.*, **104**, 31 369–31 379.

Poelman, D. R., 2014: A 10-year study on the characteristics of thunderstorms in Belgium based on cloud-to-ground lightning data. *Mon. Wea. Rev.*, **142**, 4839–4849.

Poelman, D. R., 2016: The European lightning location system EUCLID – Part 2: Observations. *Nat. Hazards Earth Syst. Sci.*, **16**, 607–616.

Poelman, D. R., 2024: Eleven years of total lightning insights from Belgium's ground-based lightning location system BELLS. *37th Int. Conf. on Lightning Protection (ICLP 2024)*, Dresden, Germany. [Available online at https://www.meteo.be/uploads/media/66d1774532d6f/p223-poelman.pdf?v20250829-1211]

Poelman, D. R., et al., 2016: The European lightning location system EUCLID – Part 2: Observations. *Nat. Hazards Earth Syst. Sci.*, **16**, 607–616.

Schulz, W., et al., 2005: Cloud-to-ground lightning in Austria: A 10-year study using data from a lightning location system. *J. Geophys. Res.*, **110**.

Takagi, N., et al., 1986: On the occurrence of positive ground flashes. *J. Geophys. Res.*, **91**, 9905–9909.

Taszarek, M., et al., 2020a: Severe convective storms across Europe and the United States. Part I: Climatology of lightning, large hail, severe wind, and tornadoes. *J. Climate*, **33**, 10239–10261.

Taszarek, M., et al., 2020b: Severe convective storms across Europe and the United States. Part II: ERA5 environments associated with lightning, large hail, severe wind, and tornadoes. *J. Climate*, **33**, 10263–10286.

Tuomi, T., 2001: Lightning observations in Finland, 2001. *Geophysical Publications*, **55**, Finnish Meteorological Institute, 41 pp.

Van der Velde, O., et al., 2024: Thunderstorm flash rates with the Meteosat Lightning Imager (MTG-LI) compared to the Ebro Lightning Mapping Array. *AGU Fall Meeting*, Washington, D.C., 9–13 December 2024, Poster AE23A-2558. [Available online at https://agu.confex.com/agu/agu24/meetingapp.cgi/Paper/1722129]

Wapler, K., 2013: High-resolution climatology of lightning characteristics within Central Europe. *Meteorol. Atmos. Phys.*, **122**, 175–184.

Appendices

Figure A1. METAR messages from Airport Luxembourg-Findel (ELLX) for the period 22.07.2013 21:20 UTC to 23.07.2013 05:50 UTC. The wind information '00000KT' in the METAR messages indicates the period of the wind data outage. Source: OGIMET.

SA 23/07/2013 05:50->	**METAR ELLX 230550Z VRB01KT 9999 FEW020TCU SCT140 21/16 Q1015 NOSIG=**
SA 23/07/2013 05:20->	**METAR ELLX 230520Z 00000KT CAVOK 19/16 Q1015 NOSIG=**
SA 23/07/2013 04:50->	**METAR ELLX 230450Z 00000KT CAVOK 18/16 Q1015 NOSIG=**
SA 23/07/2013 04:20->	**METAR ELLX 230420Z 00000KT CAVOK 18/15 Q1015 NOSIG=**
SA 23/07/2013 03:50->	**METAR ELLX 230350Z 00000KT CAVOK 18/15 Q1015 NOSIG=**
SA 23/07/2013 03:20->	**METAR ELLX 230320Z 00000KT CAVOK 18/16 Q1015 NOSIG=**
SA 23/07/2013 02:50->	**METAR ELLX 230250Z 00000KT CAVOK 18/16 Q1015 NOSIG=**
SA 23/07/2013 02:20->	**METAR ELLX 230220Z AUTO 00000KT 9999 NDV 19/16 Q1015=**
SA 23/07/2013 01:50->	**METAR ELLX 230150Z AUTO 00000KT 9999 NDV 20/16 Q1015=**
SA 23/07/2013 01:20->	**METAR ELLX 230120Z AUTO 00000KT 9999 NDV 21/16 Q1015=**
SA 23/07/2013 00:50->	**METAR ELLX 230050Z 00000KT CAVOK 21/16 Q1015 NOSIG=**
SA 23/07/2013 00:20->	**METAR ELLX 230020Z AUTO 00000KT 9999 NDV 20/16 Q1015=**
SA 22/07/2013 23:50->	**METAR ELLX 222350Z 00000KT CAVOK 19/17 Q1015 NOSIG=**
SA 22/07/2013 23:20->	**METAR ELLX 222320Z 00000KT 9999 FEW036 BKN110 19/17 Q1015 NOSIG=**
SA 22/07/2013 22:50->	**METAR ELLX 222250Z 00000KT 9999 FEW036 BKN110 20/17 Q1015 NOSIG=**
SA 22/07/2013 22:20->	**METAR COR ELLX 222220Z 00000KT 9999 -SHRA FEW036 BKN110 20/16 Q1015 NOSIG=**
SA 22/07/2013 21:50->	**METAR ELLX 222150Z 00000KT 9999 -SHRA SCT036 BKN090 20/16 Q1017 RETS NOSIG=**
SA 22/07/2013 21:20->	**METAR ELLX 222120Z 26007KT 250V360 9999 -TSRA FEW014 FEW030CB BKN090 22/14 Q1017 NOSIG=**

Table A1. Cantonal CG flash densities based on BELLS data for the period 2013–2024.

CANTONS	DENSITY (KM^{-2} YR^{-1})
ESCH-SUR-ALZETTE	0.56
MERSCH	0.56
DIEKIRCH	0.53
REDANGE	0.51
VIANDEN	0.51
CLERVAUX	0.50
LUXEMBOURG	0.50
WILTZ	0.49
CAPELLEN	0.47
ECHTERNACH	0.46
GREVENMACHER	0.43
REMICH	0.38

Table A2. Communal CG flash densities based on BELLS data for the period 2013–2024.

COMMUNES	DENSITY (KM^{-2} YR^{-1})
SCHIFFLANGE	0.76
DUDELANGE	0.74
LORENTZWEILER	0.72
HEFFINGEN	0.71
WALFERDANGE	0.67
WEISWAMPACH	0.66
ESCH-SUR-ALZETTE	0.66
COLMAR-BERG	0.66
MONDERCANGE	0.66
BISSEN	0.65
STEINSEL	0.64
FEULEN	0.62
ESCH-SUR-SÛRE	0.60
SAEUL	0.60
VICHTEN	0.60
USELDANGE	0.60
RECKANGE-SUR-MESS	0.60
LUXEMBOURG	0.58
BOURSCHEID	0.58
BETTENDORF	0.57
VIANDEN	0.57
MERTZIG	0.57

MERSCH	0.57
RUMELANGE	0.55
PÉTANGE	0.55
SCHIEREN	0.54
ERPELDANGE	0.54
VALLÉE DE L'ERNZ	0.53
NOMMERN	0.53
BECKERICH	0.53
BETTEMBOURG	0.53
KÄERJENG	0.53
REDANGE	0.52
LAC DE LA HAUTE-SURE	0.52
LINTGEN	0.52
PUTSCHEID	0.51
STRASSEN	0.51
DIPPACH	0.51
ROESER	0.51
FRISANGE	0.51
BOULAIDE	0.51
CONSDORF	0.51
RAMBROUCH	0.51
BECH	0.51
GARNICH	0.50
JUNGLINSTER	0.50
CLERVAUX	0.50
PARC HOSINGEN	0.50
KAYL	0.50
DIFFERDANGE	0.49
TANDEL	0.49
ETTELBRUCK	0.49
WINCRANGE	0.49
KOPSTAL	0.49
HELPERKNAPP	0.49
LEUDELANGE	0.48
BIWER	0.48
FISCHBACH	0.48
SANEM	0.47
GOESDORF	0.47
PRÉIZERDAUL	0.47
KIISCHPELT	0.47
HEINERSCHEID	0.47
ROSPORT-MOMPACH	0.46
CONTERN	0.46

SANDWEILER	0.46
BEAUFORT	0.46
LAROCHETTE	0.45
BERDORF	0.45
NIEDERANVEN	0.45
WINSELER	0.45
ELL	0.45
DIEKIRCH	0.45
HESPERANGE	0.45
KEHLEN	0.44
STEINFORT	0.44
WALDBILLIG	0.43
GREVENMACHER	0.43
FLAXWEILER	0.43
BETZDORF	0.43
BERTRANGE	0.42
GROSBOUS-WAHL	0.47
WEILER-LA-TOUR	0.42
TROISVIERGES	0.41
KOERICH	0.41
LENNINGEN	0.40
MONDORF-LES-BAINS	0.40
ECHTERNACH	0.40
SCHUTTRANGE	0.40
BOUS-WALDBREDIMUS	0.43
MANTERNACH	0.38
DALHEIM	0.38
WILTZ	0.38
REMICH	0.37
MAMER	0.37
STADTBREDIMUS	0.37
SCHENGEN	0.36
MERTERT	0.34
REISDORF	0.32
WORMELDANGE	0.29

Table A3. Top 10 CG lightning days in Luxembourg based on BELLS data for the period 2013–2024.

DATE	NUMBER OF CG FLASHES
29-APR-2018	752
19-JUN-2013	685
09-JUN-2018	546
14-MAY-2018	459
04-JUL-2018	427
20-JUN-2013	405
05-SEP-2024	386
05-JUN-2019	356
07-AUG-2018	335
29-JUN-2024	308

Table A4. Results of the empirical CG flash statistics for the perimeter of the Luxembourg-Findel Airport (PMF: probability mass function, CDF: cumulative density function). The return period is given in years.

K	PMF	CDF	EXCEEDANCE	RETURN PERIOD
0	0.167	0.167	1.000	1.0
1	0.167	0.333	0.833	1.2
2	0.000	0.333	0.667	1.5
3	0.333	0.667	0.667	1.5
4	0.083	0.750	0.333	3.0
5	0.083	0.833	0.250	4.0
6	0.000	0.833	0.167	6.0
7	0.000	0.833	0.167	6.0
8	0.000	0.833	0.167	6.0
9	0.000	0.833	0.167	6.0
10	0.000	0.833	0.167	6.0
11	0.000	0.833	0.167	6.0
12	0.000	0.833	0.167	6.0
13	0.000	0.833	0.167	6.0
14	0.000	0.833	0.167	6.0
15	0.000	0.833	0.167	6.0
16	0.000	0.833	0.167	6.0
17	0.083	0.917	0.167	6.0
18	0.000	0.917	0.083	12.0
19	0.000	0.917	0.083	12.0
20	0.000	0.917	0.083	12.0
21	0.000	0.917	0.083	12.0
22	0.083	1.000	0.083	12.0